

# Water-in-Oil Pickering Emulsions Stabilized by Synergistic Particle–Particle Interactions

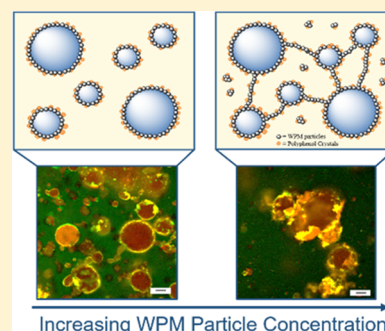
Morfo Zembyla,<sup>†</sup> Aris Lazidis,<sup>‡</sup> Brent S. Murray,<sup>\*,†</sup> and Anwesha Sarkar<sup>\*,†</sup>

<sup>†</sup>Food Colloids and Bioprocessing Group, School of Food Science and Nutrition, University of Leeds, Leeds LS2 9JT, U.K.

<sup>‡</sup>Nestlé Product Technology Centre York, P. O. Box 204, Haxby Road, York YO91 1XY, U.K.

## S Supporting Information

**ABSTRACT:** Here, we report a novel “double Pickering stabilization” of water-in-oil (W/O) emulsions, where complex formation at the interface between Pickering polyphenol particles adsorbing from the oil side and whey protein microgel (WPM) particles coadsorbing from the aqueous side of the interface is investigated. The interfacial complex formation was strongly dependent on the concentration of WPM particles. At low WPM concentrations, both polyphenol crystals and WPM particles are present at the interface and the water droplets were stabilized through their synergistic action, while at higher concentrations, the WPM particles acted as “colloidal glue” between the water droplets and polyphenol crystals, enhancing the water droplet stability for more than 90 days and prevented coalescence. Via this mechanism, the addition of WPM up to 1 wt % gave a significant improvement in the stability of the W/O emulsions, allowing an increase to a 20 wt % water droplet fraction. The evidence suggests that the complex was probably formed due to electrostatic attraction between oppositely charged polyphenol Pickering particles on the oil side of the interface and WPM Pickering particles mainly on the aqueous side of the interface. Interfacial shear viscosity measurements and monolayer (Langmuir trough) experiments at the air–water interface provided further evidence of this strengthening of the film due to the synergistic particle–particle complex formation at the interface.



## INTRODUCTION

The stabilization of emulsions by solid particles has gained significant attention during the last two decades due to their ability to irreversibly adsorb at the interface, providing kinetic stability to the dispersed phase.<sup>1,2</sup> Such solid particles are known as “Pickering” particles and tend to hinder coalescence by virtue of their exceptionally high desorption energies that make the particles practically impossible to desorb once adsorbed.<sup>3</sup> Besides oil-in-water (O/W) emulsions, Pickering stabilization has gained increased research attention among colloid scientists for stabilizing water-in-oil (W/O) emulsions owing to the limited number of biocompatible water-insoluble particles being investigated to stabilize water droplets to date, such as fat crystals, polyphenol crystals, etc.<sup>2–4</sup>

In addition to single particle-laden interfaces, there has been growing interest in stabilizing emulsions by dual or hybrid particles. When two oppositely charged colloidal particles are used, the ability of particles to adsorb at the water–oil interface depends on mutual interactions between these two particles.<sup>5</sup> For an emulsion drop to be stable, sufficient packing of particles at the interface is necessary to prevent coalescence and subsequent phase separation.<sup>5</sup> For example, droplets have been shown to be stabilized by an electrostatic complex of lactoferrin nanogel particles and inulin nanoparticles, where the particles form particle–particle complexes at the interface and provide better coverage and consequently more stability.<sup>6</sup> However, such studies are relatively rare in the W/O emulsion domain. Nallamilli et al.<sup>7,8</sup> stabilized W/O emulsions using a

combination of silica and polystyrene particles. The silica particles were more hydrophilic and sited toward the water phase, while polystyrene particles were more hydrophobic and protruded outward into the oil phase, located above the silica particle layer. Pushpam et al.<sup>5</sup> also showed that oppositely charged colloids can stabilize W/O emulsions by controlling the charge ratio and the number of particles on their surfaces. In addition, they have investigated the influence of the charge ratio on the structural arrangement of particles or in the pattern formation at the emulsion interface.<sup>5</sup>

In our previous work, we have shown the ability of water-insoluble polyphenol crystals such as curcumin and quercetin to stabilize water droplets via the Pickering mechanism.<sup>2</sup> Microstructural evaluation at various length scales revealed that quercetin crystals had a more rodlike shape than curcumin crystals, the latter being smaller and having a more polyhedral shape.<sup>2</sup> It was observed that such polyphenol crystals adsorb at the interface and provide stabilization of water droplets for several days. However, the formation of a hybrid polyphenol–whey protein isolate (WPI) complex at the water–oil interface revealed a pronounced improvement in the kinetic stability.<sup>4</sup> This complex formation was produced between the Pickering polyphenol particles adsorbing from the oil side and free molecules of biopolymer (WPI protein) coadsorbing from the

Received: July 1, 2019

Revised: September 11, 2019

Published: September 17, 2019

aqueous side of the interface, which strengthened the mechanical properties of the adsorbed film.<sup>4</sup> It was also suggested that this complex strengthening was due to an electrostatic attraction between the oppositely charged polyphenol particles and protein at the interface, although hydrogen bonding between the two components may also contribute.<sup>4</sup> Although the complexes improved stability, above 5 wt % water, the emulsions still exhibited some coalescence over several weeks. Therefore, to engineer interfaces of W/O emulsions with enhanced performance, one novel strategy would be to investigate if W/O emulsions could be stabilized by complex formation between two Pickering stabilizers, namely, the same polyphenol particles combined with protein-based microgel particles, rather than protein molecules. To our knowledge, the use in this way of such combined biocompatible Pickering stabilizers remains uninvestigated.

Protein microgels are soft colloidal particles that can be produced using a top-down technique of forming a physically cross-linked heat-set hydrogel in the first stage. Then, microgel particles are produced by breaking the gel down under high shear forces using a homogenizer.<sup>9</sup> Whey protein microgel (WPM) particles result from controlled shearing of a heat-set gel formed via the disulfide bonding between  $\beta$ -lactoglobulin ( $\beta$ -lg) and  $\alpha$ -lactalbumin ( $\alpha$ -la) molecules, as well as between the same proteins.<sup>10</sup> Upon heat denaturation at 90 °C, the unfolded whey proteins expose hydrophobic residues and thiol groups and start to aggregate. The initially quick formation of small primary aggregates is followed by fractal aggregation, which leads to the formation of larger particles that are primarily held together by hydrophobic and hydrogen bonds.<sup>10,11</sup> Subsequently, intraparticle disulfide bonds are formed, leading to covalent stabilization of the structure.<sup>10,11</sup> A combination of steric and electrostatic repulsion confers good colloidal stability to these microgels in aqueous dispersions.<sup>12</sup>

In this work, we show a unique stabilization mechanism for W/O emulsions, containing up to 20 wt % water, via interfacial complex formation between the same curcumin or quercetin polyphenol crystals and WPM particles. It is hypothesized that polyphenol crystals coming from the continuous (oil) phase and WPM particles in the aqueous phase form complexes at the interface via the same attractive electrostatic and/or hydrogen-bonding interactions as observed earlier for non-microgel (molecular) WPI but, in this case, forming a sort of “double Pickering stabilization”. The stability of the corresponding W/O emulsion droplets was evaluated as a function of different WPM particle concentrations, and the mechanism of the interfacial interactions was probed using a range of complimentary physical and microstructural techniques.

## MATERIALS AND METHODS

**Materials.** Curcumin (orange-yellow powder) from turmeric rhizome (96% total curcuminoid content) was obtained from Alfa Aesar (U.K.). Quercetin ( $\geq 95\%$ ) in the form of a yellow crystalline solid was purchased from Cayman Chemicals. Both the polyphenol crystals were used without further purification. Soybean oil (KTC Edibles, U.K.) was purchased from a local store. Aluminum oxide (99%, extra pure) was used for soybean oil purification in some experiments and was purchased from Acros Organics (Belgium). Whey protein isolate (WPI) containing 96.5% protein was obtained from Fonterra (New Zealand). Water, purified by treatment with a Milli-Q apparatus (Millipore, Bedford, U.K.), with a resistivity not less than 18 M $\Omega$  cm<sup>-1</sup>, was used for the preparation of the emulsions. A few drops of hydrochloric acid (0.1 M HCl) or sodium hydroxide (0.1

M NaOH) were used to adjust the pH of the emulsions. *n*-Hexane (99%) was obtained from Alfa Aesar (U.K.). Sodium azide and rhodamine B were purchased from Sigma-Aldrich.

**Preparation of Aqueous Dispersion of Whey Protein Microgel (WPM) Particles.** An aqueous dispersion of WPM particles was prepared based on a slight modification of the methods previously described by Murray and Phisarnchananan<sup>13,14</sup> via the disulfide-bond-mediated covalent cross-linking of WPI followed by controlled shearing. Whey protein solution (10 wt %) was prepared by dissolving WPI powder in a 20 mM phosphate buffer solution at pH 7.0 for 2 h. The WPI solution was then heated at 90 °C for 30 min and cooled down at room temperature for 30 min followed by storage at 4 °C overnight to form whey protein hydrogels. The gels were mixed with a 20 mM phosphate buffer solution (1:1 w/w) at pH 7.0 and prehomogenized using a blender (HB711M, Kenwood, U.K.) for 3 min before homogenization using two passes through the Leeds Jet homogenizer (University of Leeds, U.K.) operating at a pressure of 300  $\pm$  20 bar. Sodium azide (0.02 wt %) was added to the final 5 wt % WPM stock solution.

**Particle Size Measurement of WPM Particles.** The mean hydrodynamic diameter ( $d_H$ ) of the WPM particles at pH value 3 was measured by dynamic light scattering at 25 °C via a Malvern Zetasizer Nano-ZS instrument (Malvern Instruments, Worcestershire, U.K.). Assuming WPM particles to be spherical, the apparent particle diameter was calculated from the measured diffusion coefficient ( $D$ ) via the Stokes–Einstein equation

$$d_H = \frac{k_b T}{3\pi\eta D} \quad (1)$$

where  $k_b$  is the Boltzmann constant,  $T$  is the temperature, and  $\eta$  is the viscosity of the solution.

Particle sizes were measured after diluting the samples to 0.5 wt % with 20 mM phosphate buffer. The pH was adjusted to 3.0 or 7.0 by adding a few drops of 0.1 M HCl or NaOH. Solution (1 mL) was injected into a clean cuvette (poly(methyl methacrylate), Brand GmbH, Wertheim, Germany). The refractive index of WPM particles and the dispersion medium were set at 1.545 and 1.33, respectively. The absorbance of the protein was assumed to be 0.001. The hydrodynamic diameters ( $d_H$ ) were calculated by the cumulant analysis method of the autocorrelation function from the Zetasizer software.

**Electrophoretic Mobility.** The  $\zeta$ -potential and electrophoretic mobility measurements of WPM particles in the aqueous phase and polyphenol crystals dispersed into the soybean oil phase were performed using the Malvern Zetasizer Nano-ZS instrument. The WPM dispersion was diluted to 0.5 wt % using phosphate buffer solution (20 mM). The pH was adjusted to 3.0 or 7.0 by adding a few drops of 0.1 M HCl or NaOH. It was then added to a folded capillary cell (model DTS 1070, Malvern Instruments Ltd., Worcestershire, U.K.). Curcumin and quercetin crystals (0.14 wt %) were dispersed in the continuous phase (soybean oil) using an Ultra-Turrax T25 mixer (Janke & Kunkel, IKA-Labortechnik) with a 13 mm mixer head (S25N-10G) operating at 9400 rpm for 5 min. The larger crystals were left to sediment for 2 h at room temperature, and then the top layer was added to a cuvette (model PCS 1115, Malvern Instruments Ltd., Worcestershire, U.K.) where a universal “dip” cell (model Zen 1002, Malvern Instruments Ltd., Worcestershire, U.K.) was used for measuring the mobility in nonaqueous systems.

For the WPM, the instrument software was used to convert the electrophoretic mobility into  $\zeta$ -potential values using the Smoluchowski or Hückel approximation for WPM particles. The  $\zeta$ -potential was calculated from the measured electrophoretic mobility using Henry's equation

$$\mu = \frac{\zeta \epsilon_r \epsilon_0 f(\kappa a)}{\eta} \quad (2)$$

where  $\zeta$  is the zeta potential,  $\kappa a$  is the reduced inverse Debye length, and  $\eta$  is the viscosity of the solvent. The value of  $f(\kappa a)$  is determined by the medium, the electrolyte concentration, and the size of the

colloids. In aqueous systems where  $\kappa\alpha \gg 1$ ,  $f(\kappa\alpha) = 1$  (Smoluchowski limit), whereas for nonaqueous systems,  $\kappa\alpha \ll 1$  and  $f(\kappa\alpha) = 2/3$  (Hückel limit). Hence, mobilities in nonaqueous systems (relevant for curcumin or quercetin) are greatly reduced<sup>15</sup> compared to those in aqueous systems (relevant for WPM) due to the lower dielectric constant of the medium and in this case the higher viscosity of the oil ( $57.1 \pm 1.1$  mPa·s<sup>16</sup>).

**Preparation of W/O Emulsions.** Curcumin or quercetin dispersions were prepared by dispersing the polyphenol crystals (0.14 wt %) in the continuous phase (soybean oil) using an Ultra-Turrax T25 mixer (Janke & Kunkel, IKA-Labortechnik) with a 13 mm mixer head (S25N-10G) operating at 9400 rpm for 5 min. The stock WPM solution (5 wt %) was diluted to the desired WPM concentration (0.05–2.0 wt %) and used as the aqueous phase. The pH of the aqueous phase was adjusted to 3.0 or 7.0, depending on the experiment, by adding a few drops of 0.1 M HCl or NaOH. Coarse W/O emulsions were prepared by homogenizing 10, 20, 30, or 50 wt % of this aqueous phase with soybean oil in an Ultra-Turrax mixer for 2 min at 13 400 rpm. Fine emulsions were prepared by passing the coarse emulsions through a high-pressure Leeds Jet homogenizer, twice, operated at  $300 \pm 20$  bar. The initial temperature of the particle dispersion was 21 °C. The temperatures of the dispersions were 23 and 26 °C after Ultra-Turrax-mixing at 9400 rpm for 5 min and 13 400 rpm for 2 min, respectively. The temperature of the dispersions after passing through the Jet homogenizer (two passes at  $300 \pm 20$  bar) was 33–34 °C. Note that these slight temperature increases were too low to have any significant impact on the solubility of the particles or the proteins.<sup>2</sup> Immediately after preparation, emulsions were sealed in 25 mL cylindrical tubes (internal diameter = 17 mm) and stored at room temperature in a dark place.

**Droplet Size Measurement of Emulsions.** The particle size distributions (PSDs) of emulsions were measured using static light scattering via a Mastersizer Hydro SM small volume wet sample dispersion unit (Malvern Instruments, Worcestershire, U.K.). The average droplet size was monitored via the Sauter mean diameter,  $D_{3,2}$ , or volume mean diameter,  $D_{4,3}$ , defined by

$$D_{ab} = \frac{\sum n_i d_i^a}{\sum n_i d_i^b} \quad (3)$$

where  $n_i$  is the number of the droplets of diameter  $d_i$ .

For water droplet size measurements, refractive indices of 1.33 and 1.47 were used, for water and soybean oil, respectively. Absorption coefficients of 0.01, 0.1, and 0.01 for curcumin, quercetin, and water were used, respectively. All measurements were made at room temperature on at least three different samples.

**Confocal Laser Scanning Microscopy.** The microstructure of the W/O emulsions was observed using a confocal microscope (Zeiss LSM700 inverted, Germany). Approximately, 80  $\mu$ L of sample was placed into a laboratory-made well slide and a coverslip (0.17 mm thickness) was placed on top, ensuring that there was no air gap (or bubbles) trapped between the sample and coverslip. The samples were scanned at room temperature ( $25 \pm 1$  °C) using a  $20 \times 0.5$  objective lens. Autofluorescence from the particles was excited using 488 and 405 nm lasers for curcumin and quercetin crystals, respectively. Rhodamine B was used as a dye for whey protein and added before the confocal analysis in all cases. It was excited using 545 nm lasers. The emitted fluorescent light was detected at 525, 460, and 580 nm for curcumin, quercetin, and rhodamine B, respectively.

**Langmuir Trough Measurements.** A specialist Langmuir trough featuring a rhombic poly(tetrafluoroethylene) barrier, described in detail elsewhere,<sup>17–20</sup> was used throughout this work. The surface pressure was measured by the Wilhelmy plate method, using a thoroughly cleaned, roughened mica plate (3–5 cm in length), which was suspended in the middle of the trough from a sensitive force transducer (Maywood Instruments, Basingstoke, U.K.). Before WPM particles or polyphenol crystals were spread, the air–water (A–W) interface was reduced rapidly to an area lower than that used in the subsequent  $\pi$ –A experiments. The interface was sucked clean with a vacuum line, the interface expanded, and the process repeated until  $\pi$

< 0.1 m N m<sup>-1</sup> was obtained on compression. For spreading from organic solvent (hexane), a drop of the spreading solution was slowly formed on the tip of the syringe, and then the drop was slowly lowered to touch the interface, the syringe tip raised, and the process repeated until all of the solution had been spread. For the WPM particle experiments, 50  $\mu$ L of a 0.3 wt % WPM particle suspension (in Milli-Q water, pH 3.0) was spread at the A–W interface (aqueous phase at pH 3.0). For the polyphenol crystal experiments, concentrations of 0.5 wt % curcumin or 0.9 wt % quercetin in hexane were prepared, and the mixture was sonicated for 1 min using a high-intensity ultrasonic probe (Sonics & Materials Inc., Newton, CT) while sparging with air. Then, 100  $\mu$ L of these hexane mixtures were spread at the A–W interface (aqueous phase at pH 3.0). Spreading took 1–2 min and measurement of the  $\pi$ –A isotherm was begun 10 min after spreading, after which all of the hexane had evaporated. For the experiments where both polyphenol crystals and WPM particles were spread at the interface, polyphenol suspensions in hexane were spread first (100  $\mu$ L) and then the system was left for 10 min to allow the solvent to evaporate before adding the WPM particle suspension (50  $\mu$ L) as before. The system was then left for another 10 min to help ensure that both components were evenly dispersed throughout the interface. Films were compressed at a constant low speed, as described previously,<sup>17–20</sup> such that the rate of relative change in area was practically linear at  $1.5 \times 10^{-4}$  s<sup>-1</sup> for the isotherms recorded.

**Interfacial Shear Viscosity ( $\eta_i$ ).** A two-dimensional Couette-type interfacial viscometer, described in detail elsewhere,<sup>21,22</sup> was operated in a constant shear rate mode to measure interfacial viscosity. Briefly, a stainless steel biconical disc (radius 15.0 mm) was suspended from a thin torsion wire with its edge in the plane of the W/O interface of the solution contained within a cylindrical glass dish (radius 72.5 mm). The constant shear rate apparent interfacial viscosity,  $\eta_i$ , is given by the following equation

$$\eta_i = \frac{g_f}{\omega} K(\theta - \theta_0) \quad (4)$$

where  $K$  is the torsion constant of the wire;  $\theta$  is the equilibrium deflection of the disc in the presence of the film;  $\theta_0$  is the equilibrium deflection in the absence of the film, i.e., due to the bulk drag of the subphase on the disc;  $g_f$  is the geometric factor; and  $\omega$  is the angular velocity of the dish. A fixed value of  $\omega = 1.27 \times 10^{-3}$  rad s<sup>-1</sup> was used, which aids in comparison with measurements made on many other systems at the same shear rate.

For these measurements, 0.14 wt % curcumin or quercetin particles were dispersed in purified soybean oil using the Ultra-Turrax mixer at 9400 rpm for 5 min. The oil was purified with aluminum oxide to eliminate free fatty acids and surface-active impurities that may affect the measurements. A mixture of oil and aluminum oxide in proportion 2:1 w/w was stirred for 3 h and centrifuged at 4000 rpm for 30 min.

**Statistical Analysis.** Significant differences between samples were determined by one-way analysis of variance and multiple comparison test with Tukey's adjustment performed using SPSS software (IBM, SPSS statistics), and the level of confidence was 95%.

## RESULTS AND DISCUSSION

**Characterization of Aqueous Dispersion of WPM Particles.** The particle size distribution of the WPM dispersions as determined by dynamic light scattering was monomodal (Supporting Information Figure S1) with a polydispersity index of  $\sim 0.3$  and a mean hydrodynamic radius of  $\sim 90$  nm at either pH 3.0 or 7.0 (Table 1), i.e., there was no significant change in size at these pH values. The WPM particles display a polyampholyte character in line with their constituent proteins, with an isoelectric point (IEP) at pH 4.7, where their overall charge is zero.<sup>23</sup> Below and above this pH value, WPM particles were positively and negatively charged, respectively (Table 1), as observed previously.<sup>9,24</sup> The particles are stable against aggregation when the  $\zeta$ -potential exceeds the

**Table 1. Size and  $\zeta$ -Potential of 0.5 wt % WPM Particles in the Aqueous Phase at pH Values 3.0 and 7.0**

	pH 3.0	pH 7.0
size/nm	90.4 $\pm$ 0.7	91.4 $\pm$ 0.5
$\zeta$ -potential/mV	+24.5 $\pm$ 1.1	-24.3 $\pm$ 0.4
mobility/ $\mu\text{m cm V}^{-1} \text{s}^{-1}$	+1.9 $\pm$ 0.1	-1.9 $\pm$ 0.0

absolute value of 20 mV.<sup>11</sup> The overall charge and the colloidal stability of these particles are a result of a balance between the dissociation of carboxylic and amino groups of the whey protein side chains as a function of pH.<sup>11</sup>

The attachment of WPM particles to the interface must differ from that exhibited by solid particles.<sup>25</sup> In Pickering emulsions, the contact angle of the solid particle surface at the oil–water interface is fixed and can be used to predict the type of the emulsion (oil-in-water or water-in-oil) and the particle adsorption strength.<sup>26</sup> However, for a microgel system, the particles are deformable and porous and to think in terms of a particle contact angle is misleading.<sup>27</sup> Consequently, it is not easy to properly define a line of contact between the pair of immiscible liquids and the particle surface.<sup>28</sup> Due to the conformational flexibility of its dangling chains, the location of the adsorbed microgel particle is characterized, not so much by a sharp particle–fluid interface but rather by a continuous polymer density profile.<sup>28</sup>

**Characterization of Polyphenol Particles in the Oil Phase.** Particle charging in nonaqueous liquid suspensions has received increasing attention due to enhanced technological interest.<sup>29,30</sup> Electric charges and surface potentials depend not only on the nature of solid particles but also on the nature of suspension liquid and on the soluble residues (potential determining ions, impurities, etc.).<sup>29,31</sup> Large particles are suspended more readily than the smaller ones. Therefore, they tend to appear as characteristic clusters.<sup>29</sup> Van der Waals forces acting between the particles have been supposed to control their aggregation. However, these forces depend only slightly on the nature of the oil.<sup>31</sup>

Surface charging in nonaqueous suspensions is considered to occur through:<sup>29</sup>

- Electron transfer due to extreme Lewis type of electron acceptor (acid)–electron donor (base) interactions.
- Proton transfer due to extreme Brønsted type of hydrogen bond (acid–base) interactions. This is typical in the presence of moisture, which results in the dissociation of surface hydroxyl groups and dissolution of ions as solvated complexes.
- Adsorption of surface-active solutes (surfactants), ion transfer of dissolved ions, or the presence of liquid or solid impurities.

The electrophoretic mobility results for curcumin and quercetin crystals dispersed in the oil phase are shown in Table 2. Different applied voltages were tested to determine the most reproducible results. It was determined that at higher voltages (>80 V), the phase plots and the mobility results were more reproducible (results are not shown), and the results at

**Table 2. Mobility of 0.14 wt % Polyphenol Crystals in the Oil Phase (at 150 V)**

	curcumin crystals	quercetin crystals
mobility/ $\mu\text{m cm V}^{-1} \text{s}^{-1}$	-0.0031 $\pm$ 0.0009	-0.0035 $\pm$ 0.0002

an applied voltage of 150 V are shown in Table 2. Partly due to the very high viscosity ( $57.1 \pm 1.1 \text{ mPa}\cdot\text{s}^{16}$ ) of the soybean oil, the mobility of the particles is expected to be low. Both polyphenol crystals showed a small negative mobility value indicating the presence of some negative charge at the particle surface when they are dispersed in the oil. This validates the hypothesis of attractive electrostatic interactions at the W/O interfaces between the slightly anionic polyphenol crystals in the oil and cationic WPM in the aqueous phase at pH 3.0 (Table 1).<sup>4</sup> Since converting mobilities to  $\zeta$ -potentials in nonpolar media<sup>30,31</sup> can be complicated, involving lot of unknowns, we have chosen not to do this conversion, since the main objective of this experiment was to confirm the sign (negative or positive) of any charge on the particles.

**W/O Pickering Emulsions Stabilized by WPM–Polyphenol Crystal Complexes. Stability of W/O Emulsions as a Function of WPM Particle Concentration.** The particle size distribution (PSD) of the W/O emulsions, prepared at pH 3.0 with 0.14 wt % curcumin or quercetin crystals dispersed in the oil phase and different concentrations of WPM particles in the aqueous phase, are shown in Figure 1(a),(b), respectively. A small peak below 1  $\mu\text{m}$  was observed in all of the emulsions, most likely due to some WPM aggregates or WPM–polyphenol particle complexes dispersed into the bulk oil phase by the very high shear fields. The initial size ( $D_{3,2}$  values) of the water droplets stabilized by curcumin crystals decreased from 23 to 20  $\mu\text{m}$  as the concentration of WPM particles increased from 0.05 to 2.0 wt %, respectively. Over time, the  $D_{3,2}$  values of curcumin systems containing 0.05 and 0.1 wt % WPM particles increased significantly (from  $\sim$ 22 to  $\sim$ 32  $\mu\text{m}$ ,  $p < 0.05$ ; see Supporting Information Table S1) as shown in Figure 1(b), and the emulsions with curcumin +0.05 wt % WPM particles formed even larger water droplets, with a clear water layer being observed after 21 days. On the other hand, the size of the water droplets containing 0.1, 0.5, 1.0, and 2.0 wt % WPM particles was stable ( $p > 0.05$ ; see Supporting Information Table S1), for more than 90 days (Figure 1(b)). The  $D_{3,2}$  values of the systems containing quercetin were stable ( $\sim$ 20  $\mu\text{m}$ ) for all of the concentrations of WPM particles for more than 21 days, except for the lowest WPM concentration (0.05 wt %), where the size of the water droplets increased significantly ( $p < 0.05$ ; see Supporting Information Table S2) and they phase-separated within 2 weeks (Figure 1(b<sub>ii</sub>)). The emulsions containing quercetin +0.1 and 0.5 wt % WPM particles were stable for 21 days, whereas those with 1.0 and 2.0 wt % WPM particles were stable for more than 90 days ( $p > 0.05$ ; see Supporting Information Table S2) and no clear water layer observed after this time. The curcumin systems were even stable for >90 days at WPM concentrations >0.1 wt %, probably due to the smaller size ( $D_{3,2} \sim 0.2 \mu\text{m}$ )<sup>2</sup> and lower aspect ratio of the curcumin crystals, allowing greater coverage of the interface (as observed in the confocal images, Figure 2a) as noted previously.<sup>2,4</sup> The quercetin crystals have a more rodlike shape and larger mean size ( $D_{3,2} \sim 5.9 \mu\text{m}$ ).<sup>2</sup>

The sizes of the water droplets for both the curcumin and quercetin systems with WPM, though stable, were apparently larger than those obtained in our previous work with just the polyphenols,<sup>2</sup> though it should be remembered that the light scattering technique used cannot distinguish between water droplets, polyphenol crystals, WPM particles, or their aggregates as scattering centers.<sup>32</sup> Although the apparent larger droplet size suggests that the WPM inhibited the stabilization by the polyphenols or caused the water droplets to aggregate

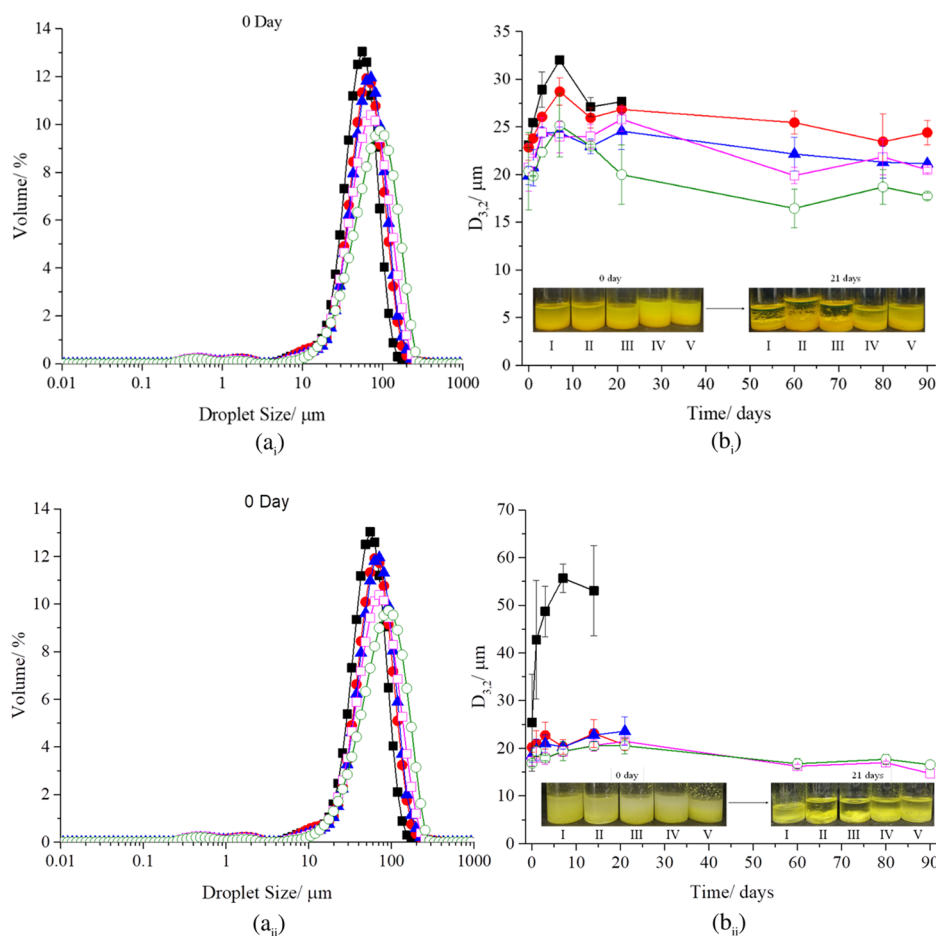


**Figure 1.** Droplet size distribution (a) and mean droplet size ( $D_{3,2}$ ) of water droplets over time with visual images (b) of 10 wt % W/O emulsions stabilized by 0.14 wt % curcumin (i) and quercetin (ii) crystals in the oil phase and 0.05 wt % [■] [I], 0.1 wt % [red ●] [II], 0.5 wt % [blue ▲] [III], 1.0 wt % [pink □] [IV], and 2.0 wt % [green ○] [V] WPM particles in the aqueous phase at pH 3.0. For statistical analysis according to Tukey's test, see Supporting Information Tables S1 and S2 for curcumin and quercetin, respectively.

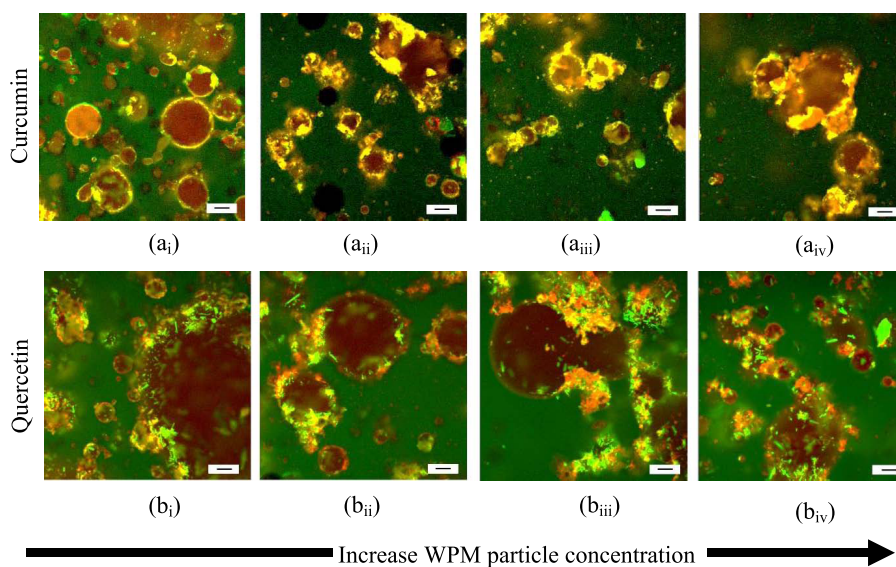


**Figure 2.** Confocal images of 10 wt % W/O Pickering emulsions stabilized by 0.14 wt % curcumin (a) and quercetin (b) crystals in the oil phase and different concentrations of WPM particles in the aqueous phase: 0.1 (i), 0.5 (ii), 1.0 (iii), and 2.0 wt % (iv) for freshly prepared samples. The green brightness in the images is caused by the autofluorescence of curcumin (488 nm excitation) or quercetin (405 nm excitation) crystals. The red brightness is due to the WPM particles stained by rhodamine B (568 nm excitation). The scale bar represents 50  $\mu\text{m}$ .

more, in the previous work<sup>2</sup> with just polyphenols, the water fraction in the emulsions was only 5 wt %, whereas here with WPM, 10 wt % water was stabilized.

Emulsions were also prepared at pH 7.0, but as previously discussed<sup>4</sup> at this pH value, the polyphenol crystals tend to degrade chemically and the emulsion stability was significantly impaired (see Supporting Information Figure S2). In any case, the results suggest that if electrostatic complex formation contributes to emulsion stability, it will be less effective at pH 7.0 because both WPM particles and the polyphenols would have the same (negative) sign of charge (Tables 1 and 2, Zembyla et al.<sup>4</sup>).

Confocal images of fresh emulsions stabilized by polyphenol crystals dispersed in the oil and different concentrations of WPM particles dispersed in the aqueous phase are shown in Figure 2. The green brightness in the images is due to the autofluorescence of the polyphenol particles. Rhodamine B (red) was used to visualize the WPM particles. As one might expect, the intensity of red color within the spherical water droplets indicates that the WPM particles preferred to be in the water phase. In line with the emulsion results indicating higher stability at higher WPM particle concentration (Figure 1), the intensity of red color at the W/O interface increased with increasing WPM concentration (Figure 2a). In the curcumin system with low concentrations of WPM particles (<0.1 wt %), the WPM particles and crystals formed a very uniform layer around the water droplets. With quercetin even at WPM particle concentrations >0.1 wt %, the adsorbed layer was less uniform, with some droplets apparently having far less than complete coverage, with an increasing tendency for the droplets to aggregate, e.g., Figure 1(b<sub>ii</sub>). As the concentration of WPM particles increased (>0.1 wt %) in both systems, there was an increased tendency for the whole system to aggregate, with WPM particles seemingly aggregated at the interface of individual droplets and between interfaces, i.e., causing flocculation of the water droplets. The polyphenol crystals seemed to be mixed in with these aggregates. In other words, as the concentration of WPM increased, there was an increased tendency for microgels to become shared between droplets.

Confocal images of aged (for 21 days) emulsions stabilized by polyphenol crystals and 2.0 wt % WPM particles are shown in Figure 3. The appearances of both the curcumin and quercetin systems seemed to have remained stable over time, and no coalescence was observed.

**Effect of Volume Fraction of Water Droplets.** Higher water:oil ratios (15, 20, and 30 wt % water) were tested for curcumin (0.14 wt %) or quercetin (0.14 wt %) crystals +2.0 wt % WPM particles as Pickering stabilizers, since this WPM particle concentration provided enhanced stability to 10 wt % W/O emulsions. Figure 4 shows that the initial  $D_{3,2}$  of the emulsions with curcumin or quercetin crystals was not significantly different ( $\sim 15 \mu\text{m}$ ,  $p > 0.05$ ; see Supporting Information Tables S3 and S4 for curcumin and quercetin, respectively) as the volume fraction increased from 15 to 20 wt %, while at 30 wt % water, the size decreased significantly in both systems. Selected images of these emulsions, shown in Figure 4, illustrate the dense and uniform coverage of the droplets by polyphenol crystals (yellow). As the wt % water increases and therefore the absolute amount of WPM particles available increases (though the WPM particle concentration remains the same), the absolute amount of polyphenol available will decrease. However, the optimum ratio of WPM particles to polyphenol to achieve the most rapid interfacial

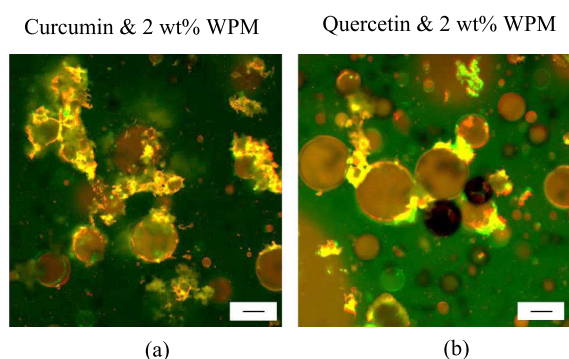


**Figure 3.** Confocal images of 10 wt % W/O Pickering emulsions stabilized by 0.14 wt % curcumin (a) and quercetin (b) crystals in the oil phase and 2.0 wt % WPM particles in the aqueous phase (pH 3.0) for 21 day old samples. The green brightness in the images is caused by the autofluorescence of curcumin (488 nm excitation) or quercetin (405 nm excitation) crystals. The red brightness is due to WPM particles stained by rhodamine B (568 nm excitation). The scale bar represents  $50 \mu\text{m}$ .

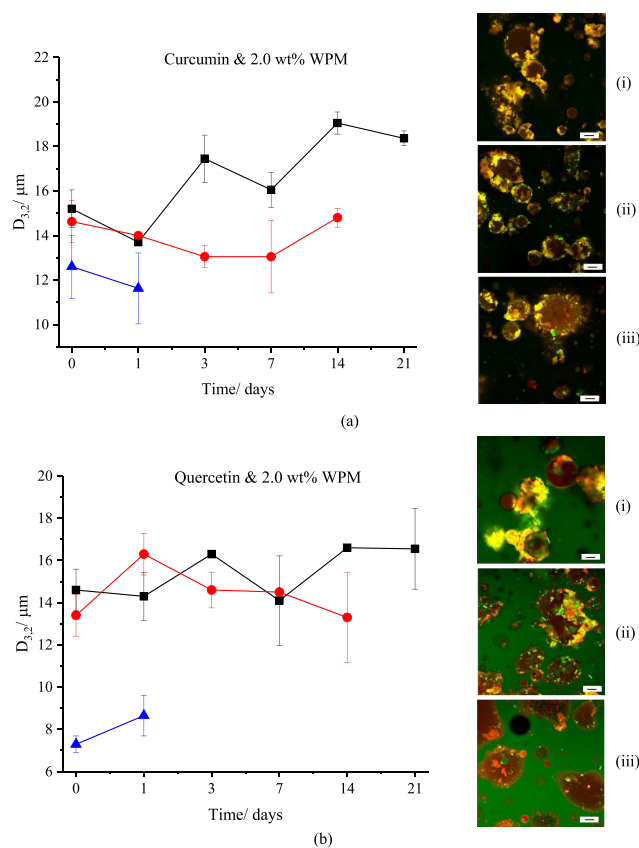


**Figure 4.** Mean size of water droplets ( $D_{3,2}$ ) over time and confocal images (i–iii) of W/O emulsions stabilized by 0.14 wt % curcumin (a) and quercetin (b) crystals containing 15 wt % (■, i), 20 wt % (●, ii), and 30 wt % (▲, iii) water with 2.0 wt % WPM particles at pH 3.0. For statistical analysis according to Tukey's test, see Supporting Information Tables S3 and S4 for curcumin and quercetin, respectively. The green brightness in the images is caused by the autofluorescence of curcumin (488 nm excitation) or quercetin (405 nm excitation) crystals. The red brightness is due to WPM particles stained by rhodamine B (568 nm excitation). The scale bar represents  $50 \mu\text{m}$ .

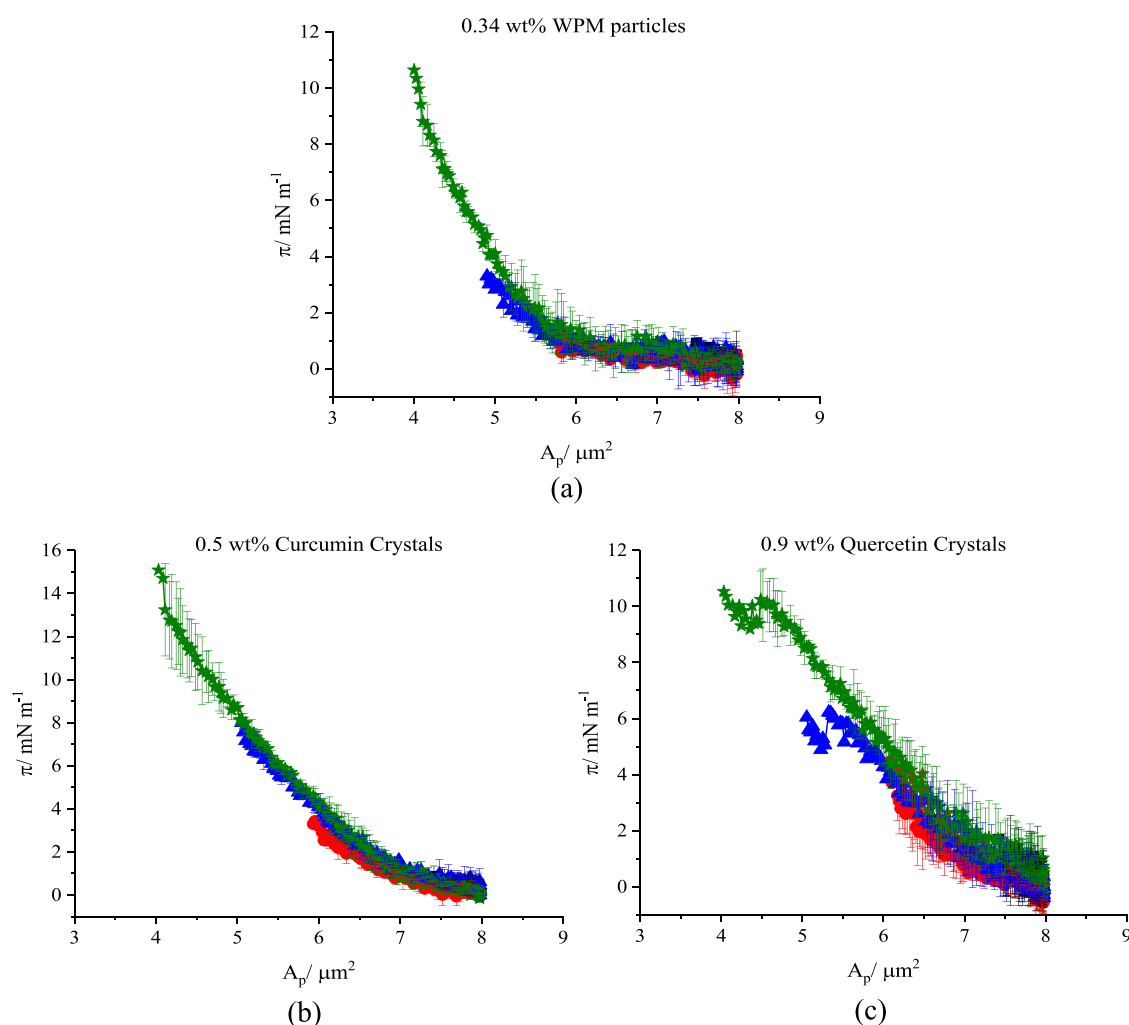


**Figure 5.** Surface pressure ( $\pi$ ) versus ( $A_p$ ) isotherms at A–W interface (aqueous phase at pH 3.0) spread solutions of 0.34 wt % WPM particles (a), 0.5 wt % curcumin (b), and 0.9 wt % quercetin (c) particles under different compression and expansion times; first compression–expansion (■), second compression–expansion (red ●), third compression–expansion (blue ▲), and fourth compression–expansion (green ★).

complex formation during emulsification is difficult to calculate, given that the two types of particle approach the interface from the two different phases. The WPM particles are generally smaller than those of the polyphenol crystals so that possibly greater WPM particle coverage in the early stages of water droplet formation aids in polyphenol coadsorption (via the various attractive interactions proposed), explaining the initial reduction in the droplet size. More efficient adsorption of both components at the interface also apparently reduced the capacity for polyphenols to aggregate in the oil phase, as also shown in the confocal images.

The emulsions containing 15 wt % water were stable for more than 90 days (results are not shown) and had much the same microscopic appearance as shown in Figure 4. The emulsions with 20 wt % stabilized by either curcumin or quercetin crystals were stable for 14 days, while for all of the emulsion systems containing 30 wt % water, a water layer at the bottom was observed after 1 day and the systems had completely phase-separated after 3 days. Thus, between 20 and 30 wt % water, the systems became increasingly unstable, probably because there were not enough polyphenol crystals to fully cover the interface. The selected images shown in Figure 4a,b of these higher wt % water systems also illustrate this increased instability in terms of larger apparent droplet sizes.

(Note that the confocal images were obtained 3–5 h after emulsion preparation, during which significant coalescence may have occurred, which did not appear in the light scattering results as the droplet size was measured only a few minutes after emulsion preparation.)

*Microgel and Polyphenol Crystal Interactions via Monolayer Experiments.* The response of the film of adsorbed material to expansion and compression of the interface is a key factor determining the ease of formation and stability of a multitude of colloidal systems.<sup>18</sup> Using Langmuir trough techniques at the air–water (A–W) interface, we sought to obtain direct evidence for specific interactions between the protein microgels and the polyphenol crystals at an interface. Working at the A–W interface was a simplification of the system compared to the W/O emulsions, but allowed reproducible spreading of material at the interface resulting in more robust conclusions. However, manual spreading at the interface can never mimic exactly the processes of adsorption/desorption and the associated rates of conformational change during emulsification. Similarly, the solvency of air is not the same as oil and the affinity of both the microgels and polyphenol crystals for the W–O and A–W interfaces is probably not the same.<sup>18</sup>

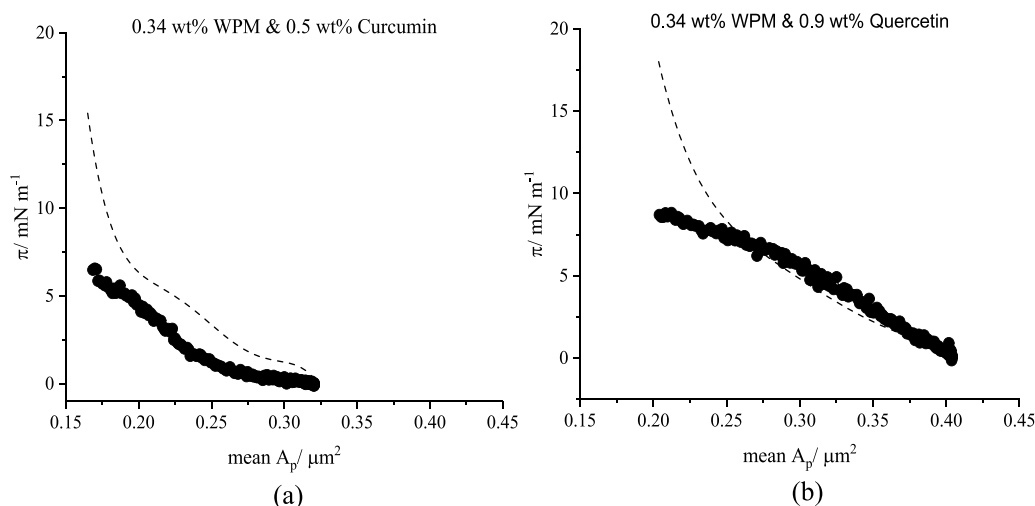


**Figure 6.** Surface pressure ( $\pi$ ) versus mean area per particle ( $A_p$ ) isotherms of mixtures of 0.34 wt % WPM particles and 0.5 wt % curcumin (a) or 0.9 wt % quercetin (b) crystals. The symbols (●) are the experimentally measured points (average of 3 runs), while the dashed lines are the theoretical results based on ideal mixing (i.e., no interactions) of WPM and curcumin or quercetin crystals.

Upon adsorption, WPM particles undergo conformational changes, which result from the balance between chain spreading, driven by surface activity, and microgel internal elasticity, promoted by cross-linking.<sup>33</sup> The extent of spreading therefore depends on various factors such as the microgel internal structure and cross-linking, their concentration, or process parameters.<sup>33</sup> Microgels tend to flatten at fluid interfaces, sometimes exhibiting a “fried egg”-like structure.<sup>34</sup> The extent of spreading has consequences for the capacity of adjacent microgels to entangle via their peripheral dangling chains, forming a two-dimensional elastic network of connected microgels.<sup>34</sup> Microgels with low deformability (highly cross-linked) barely form entanglements and fail to stabilize emulsions against mechanical disturbances. It has also been found that the conformation depends on the concentration of microgels from which they adsorb—at low concentration when the adsorption kinetics are slow, the microgels flattened, whereas at high concentrations they were more compressed laterally.<sup>33</sup> Interfaces covered with flattened microgels were adhesive, leading to bridging between adjacent interfaces, because the thin polymeric layer separating adjacent microgels could be more easily ruptured.<sup>35</sup> Thus, more deformable microgels can lead to more bridging due to their flattened conformation.<sup>36</sup> When the interfaces are covered with compressed microgels, the films are no longer adhesive because the higher polymer thickness prevents interfaces from bridging.<sup>33,35–37</sup> Other parameters such as energy input on stirring and homogenization and the size of microgels can also change the extent of spreading and thus the polymeric thickness at the interface, leading to similar consequences for bridging.<sup>33,35,37,38</sup>

Figure 5a shows the isotherms obtained by spreading a solution of 0.34 wt % WPM particles at the A–W interface at pH 3.0. Surface pressure ( $\pi$ ) is plotted against  $A_p$ , where  $A_p$  is the area per particle scaled against the cross-sectional area of the nominal particle size, i.e., a sphere of radius 45 nm (see above). This size is therefore also used to calculate the number of particles in the 0.34 wt % solution, assuming the particles have the same density as the bulk gel from which they are formed. Films were repeatedly compressed and then re-expanded and compressed again to increasingly higher

maximum  $\pi$  values to test for reversibility. It is seen that  $\pi$  starts to rise significantly at  $A_p > 1$  (somewhere between  $A_p = 7$  and 8), which may be taken as the region where the particles start to interact with each other in the interface, and thereafter  $\pi$  increases smoothly with increasing rapidity on further compression. By the time  $\pi = 10$  mN m<sup>-1</sup>, the isotherm is quite steep but  $A_p$  is still  $>4$ . This suggests that on adsorption at low  $\pi$ , the particles are significantly more expanded than their initial unadsorbed size (the maximum packing fraction for monodisperse spheres on a plane, i.e., circles, being 0.9069), and while they undergo significant compression (nearly a factor of 2 in area) up to  $\pi = 10$  mN m<sup>-1</sup>, they are still significantly expanded at this  $\pi$ . However, this assumes that the particles are monodisperse, while clearly there is a range of sizes and also probably a range of shapes so that the polydispersity of the microgels (Supporting Information Figure S1) and possibly differences in the compressibility of differently sized particles could account for some of this apparent increase in cross-sectional area. This interpretation of the isotherms also assumes that there is no irreversible desorption of particles on compression, but the reversibility and reproducibility of the isotherms, within experimental error (ca. 0.3 mN m<sup>-1</sup>), suggested that this did not take place. Particles also tended to form networks at the interface because they are attracted via capillary interactions, causing this increase of  $\pi$ . This attraction between the particles helps rendering stability of the water droplets in the emulsion systems (explained above). Overall then, the isotherms suggest that the WPM particles have a high tendency to adsorb and unfold at the A–W interface, substantiated by the emulsion results (and also the interfacial shear rheology results—see below).

Figure 5b,c shows isotherms for curcumin and quercetin crystals, respectively, after their precipitation at the A–W interface from solution (at 0.5 and 0.9 wt % in hexane, respectively) and evaporation of the solvent. Expression of the isotherms in terms of  $A_p$  as in Figure 5a immediately presents the problem of what particle size and cross-sectional area (and number of particles spread) to use for each polyphenol. The particle size and shape of the polyphenol crystals is even less precisely known. However, for illustrative purposes, since the

main intention is to examine the behavior of the mixed WPM + polyphenol films, here we assumed that the quercetin crystals had a rectangular cross-sectional  $7 \mu\text{m} \times 1 \mu\text{m}$ , i.e., each occupied an area of  $7 \mu\text{m}^2$  at the interface, while the curcumin crystals were spheres of radius  $0.1 \mu\text{m}$  and so each occupied an area of  $\pi(0.1)^2 = 0.031 \mu\text{m}^2$ . The justification for this comes from our earlier characterization of the properties of the crystals dispersed in vegetable oil for the W/O emulsions,<sup>2,4</sup> whereas here, the materials are precipitated at the interface from hexane. Removal of the crystals floating at the interface and observations of their size and shape via microscopy did not suggest that they were significantly different. Nevertheless, in view of these approximations, not too much significance should be attached to the fact that the start of the increase in  $\pi$  begins at quite high  $A_p \approx 6$ , only slightly lower than for the WPM particles. The crystals clearly should not expand, so that this is probably explained by them having a wider range of sizes and aspect ratios than assumed. This suggests that they can interact and form a network at the interface at lower coverages than the assumed sizes predict. Irrespective of this, it is seen that the isotherms are reversible, suggesting irreversible attachment and orientation within the interface. The quercetin isotherm is slightly steeper than for curcumin. Note that the amounts of polyphenol spread were chosen to give an equivalent surface area of material as the WPM particles, based on the nondeformed particle dimensions assumed above. The absolute position on the  $A_p$  scale is not important for the reasons already discussed, but the isotherms for the individual components do allow us to compare the isotherms measured for the mixed systems with those predicted by ideal mixing. Thus, if one assumes there are no attractive or repulsive interactions between the WPM and polyphenol particles in the interface, then the surface pressures should be independent of one another and additive at the same overall trough area.

Figure 6a,b shows the measured and predicted isotherms for the combined systems of 0.34 wt % WPM + 0.5 wt % curcumin or 0.9 wt % quercetin, respectively. As indicated above, these concentrations would give equal interfacial areas of the nondeformed spread materials. Note that since both materials were initially spread at high area per particle, we have assumed that this will give them sufficient interfacial space to allow them to rearrange into the same sort of mixed configuration as eventually forms on their adsorption to the W–O interface in the emulsions, although it is very difficult to obtain direct evidence of this. The predicted isotherms are simply calculated from the addition of the isotherms in Figure 5, and we have plotted  $\pi$  against the average area per particle for both particles. It is seen that for both WPM + curcumin and WPM + quercetin, the measured isotherm for the mixed system is shifted to lower  $A_p$  at equivalent  $\pi$  in the predicted isotherm. In other words, the combined materials occupy lower areas at the same  $\pi$ , suggesting attractive interaction, or interpenetration of the crystals and microgels. In view of the above discussion of a possible attractive electrostatic interaction between the polyphenol crystals and WPM particles at the W–O interface, this perhaps not surprising, but this is nice additional support for this effect. It is also seen that the shift is most pronounced for curcumin, which is noted as having much smaller crystals and which might therefore more easily penetrate, or pack in between, the WPM particles. With quercetin, the measured and predicted isotherms are coincident, within experimental error, up until ca.  $\pi = 7 \text{ mN m}^{-1}$ , beyond which the mixed area increasingly starts to diverge to lower areas compared to that

predicted by ideal mixing. Note that qualitatively, these trends will be independent of the actual choice of particle cross-sectional areas, as long as one is consistent for the single and mixed systems. Although at present, we have no way of knowing what are the actual adsorbed (i.e., rather than spread) surface concentrations of the two components at the W/O interface in the emulsions, the monolayer results provide interesting direct evidence for an attractive interaction between WPM particles and curcumin or quercetin crystals at interfaces.

**Interfacial Shear Viscosity.** To further test for evidence of interfacial complex formation, measurements of interfacial shear viscosity ( $\eta_i$ ) were undertaken as discussed in our previous work.<sup>2,4</sup> Interfacial shear viscosity is a particularly sensitive method for monitoring any structural and compositional changes within adsorbed layers.<sup>21,39</sup> Experiments were performed with purified soybean oil to remove any low-molecular-weight surface-active components (mono- and diglycerides), which tend to lower  $\eta_i$  because they are more surface-active than proteins or particles.<sup>21</sup> Figure 7 shows the

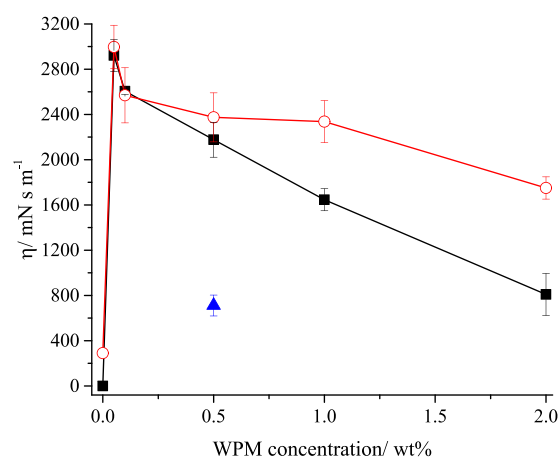


**Figure 7.** Interfacial shear viscosity at W/O interface without polyphenol crystals (only WPM particles) [blue ▲], with 0.14 wt % curcumin [■] and quercetin [red ○] crystals dispersed in purified oil with different concentrations of WPM particles in the aqueous phase after 24 h of adsorption at pH 3.0. For statistical analysis according to Tukey's test, see Supporting Information Tables S3 and S5 for curcumin and quercetin, respectively.

values of interfacial shear viscosity after 24 h in the presence of 0.14 wt % curcumin or quercetin crystals dispersed in the oil with different concentrations of WPM particles in the aqueous phase, at pH 3.0. A control experiment with purified oil (i.e., containing no polyphenol crystals) and Milli-Q water was performed but  $\eta_i = 0 \text{ mN s m}^{-1}$  even after 24 h (results are not shown). The addition of 0.5 wt % WPM particles to the aqueous phase (but with only purified oil as the continuous phase) also showed a significant increase in  $\eta_i$  reaching a maximum of  $711 \text{ mN s m}^{-1}$  after 24 h (shown as the single blue point in Figure 7).

As seen in Figure 7, for both curcumin and quercetin, the trend of  $\eta_i$  (24 h) versus WPM particle concentration at pH 3.0 was very similar. Below 0.1 wt % WPM particles, there was a significant increase of  $\eta_i$ , whereas above 0.1 wt % WPM particles,  $\eta_i$  decreased. Note that although the value for 0.5 wt % WPM particles after 24 h is high (similar to many pure globular proteins, including  $\beta$ -lactoglobulin and  $\alpha$ -lactalbumin<sup>39,40</sup>), the values for these mixed systems at low WPM

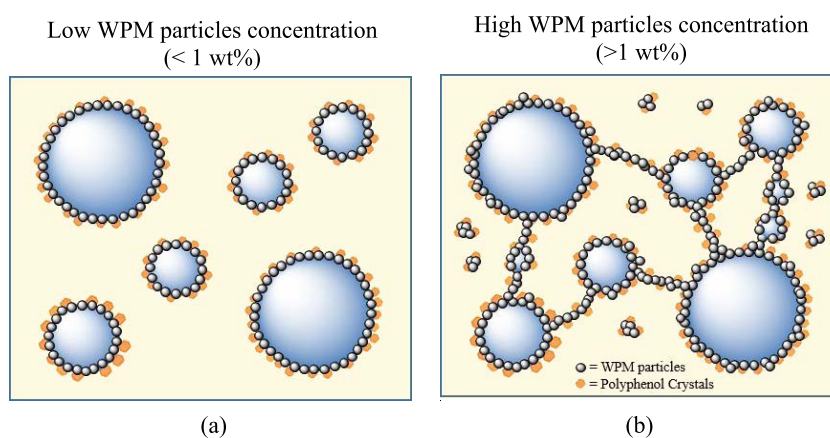


**Figure 8.** Schematic representation (not to scale) of curcumin or quercetin crystals + WPM particle-stabilized W/O emulsions, illustrating the effect of WPM particle concentration and the possible mechanism of water droplet stabilization.

particle concentration are considerably higher still. At low concentrations of WPM particles, the polyphenol crystals and WPM particles might easily coadsorb at the interface and so form complexes, giving films that are much stronger than WPM particles on their own (at 0.5 wt % WPM particles, for example). A similar effect has been identified between polyphenol crystals and WPI.<sup>4</sup> However, at higher concentrations of WPM particles, WPM adsorption will tend to dominate over crystal adsorption, and so, the  $\eta_i$  values decrease toward the values for WPM particles alone.

Curcumin gave the same  $\eta_i$  as quercetin at 0.05 and 0.1 wt % WPM particles (Figure 7), within experimental error, suggesting that both polyphenol crystals acted very similarly at lower WPM particle concentrations. However, as the concentration of WPM particles increased (>0.1 wt %),  $\eta_i$  decreased more significantly ( $p > 0.05$ ; see Supporting Information Table S5) for curcumin than for quercetin. This could be due to stronger interactions between quercetin and WPM particles, similar to the stronger interaction between quercetin and WPI suggested previously by the same  $\eta_i$  measurement.<sup>4</sup> As the WPM particle concentration was increased, more aggregated particles were present at the interface, indicating a microgel-dominated system. During the interfacial shearing, these aggregated microgels may rearrange at the interface or break down to single microgels, destroying the interfacial film, explaining the decrease of  $\eta_i$  (especially at WPM particle concentrations >0.5 wt %).

## DISCUSSION

Drawing together the results of all of these experiments, a possible mechanism of complex formation between the protein microgels and polyphenol crystals at the interface is schematically shown in Figure 8. At low concentration of WPM particles (<1 wt %), both polyphenol crystals and WPM particles coexist at the interface of the water droplets and synergistically improve the stability of the emulsions (Figure 8a). For curcumin systems, where the curcumin crystals have nearly similar shape and size as the WPM particles, both curcumin and WPM particles efficiently form complexes together, improving the water droplet coverage and stability for more than 90 days. For quercetin systems, where the quercetin crystals are much larger in size ( $D_{3,2} \sim 5.9 \mu\text{m}$ )<sup>2</sup> than WPM particles (at low concentration,  $\sim 90 \text{ nm}$ ), the complex was still formed but the water droplets were only stable for 21 days, probably due to the incomplete coverage of the water

droplets due to the larger size difference between the crystals and WPM particles. As the concentration of WPM particles increases, the size and shape of polyphenol crystals becomes less important with respect to stability. At WPM  $\geq 1.0$  wt %, the WPM particles aggregate with each other, with polyphenol crystals in the bulk phase and at the interface and between the water droplets, acting as a sort of “colloidal glue” for the whole system (Figure 8b) that immobilizes the water droplets and inhibits their coalescence. Ultimately, this synergistic action of polyphenol crystals and WPM particles is due to an electrostatic attraction between the oppositely charged polyphenol crystals and WPM particles at the interface. This depends on the pH of the aqueous phase as explained before and in our previous work,<sup>4</sup> while hydrogen bonding probably also plays a role in enhancing the interaction.

Schmitt and Ravaine<sup>41</sup> explain how the particle packing in a microgel layer can cause bridging flocculation. If the particles' packing is looser and more heterogeneous due to nonuniformity of the microgel's internal structure or limited interconnectivity with adjacent particles, then there is a tendency for microgel layers to become shared between droplets.<sup>35,41</sup> This susceptibility to bridging flocculation is considered more likely to occur in emulsions containing large stiff microgel particles having a high degree of cross-linking.<sup>35,41</sup> Another factor affecting microgel packing at the oil–water interface is the intensity of hydrodynamic disturbance during emulsification. Highly intensive shearing induces pronounced microgel flattening at the droplet surface, leading to enhanced susceptibility toward bridging flocculation.<sup>35</sup> On the other hand, a moderately low shear rate applied during emulsification favors the formation of stable droplets with surfaces fully covered by dense uniform monolayers of laterally compressed microgel particles.<sup>35</sup>

We have attempted to obtain evidence of the homogeneity of the typical arrangement (as distinct islands or mixed regions of each, for example) of the polyphenol crystals and the microgel particles at the W/O droplet interface via a range of electron microscopy (cryo-scanning electron microscopy and transmission electron microscopy) techniques. However, although the above confocal images clearly show that both components are present together, so far electron microscopy has failed to resolve the individual WPM particles at the interface, no doubt due to their more delicate nature and thus the damaging effects of dehydration, freezing, or the electron beam itself. Nor have we seen any clear evidence, with the

range of crystal sizes and shapes, of capillary interactions influencing the deformation of the interface between droplets, which for large particles has been shown to be a significant contribution to the Pickering stabilization mechanism.<sup>42</sup>

## CONCLUSIONS

In this work, we propose a novel way to stabilize W/O emulsions via a double Pickering mechanism, where polyphenol particles adsorb from the oil side and WPM particles coadsorb from the aqueous side of the interface. This complex formation was strongly dependent on the concentration of WPM particles. At low WPM particle concentrations, both polyphenol crystals and WPM particles were present at the interface, and through a synergistic action, they better stabilized the W/O emulsions. At higher WPM particle concentrations, flocculation was observed where the WPM particles acted as a colloidal glue between water droplets and polyphenol crystals enhancing the water droplet stability and preventing the coalescence. Via this mechanism, the addition of WPM particles up to 1 wt % gave a significant improvement in the stability of the emulsions up to at least 20 wt % water. It is believed that this complex formation was mainly formed due to attractive electrostatic interactions between oppositely charged polyphenol Pickering particles on the oil side of the interface and WPM Pickering particles mainly on the aqueous side of the interface, which therefore was also dependent on the pH of the aqueous phase. Interfacial shear viscosity measurements and monolayer experiments at the A–W interface provided further evidence of strengthening of the film due to the complex formation at the interface. However, higher concentrations of WPM particles do not improve the stability further due to WPM particle adsorption dominating over polyphenol particle adsorption. Combinations of such polyphenol crystals + microgels to form interfacial synergistic Pickering particle–particle complexes could be used more widely for designing water-in-oil emulsions for a variety of soft matter applications.

## ASSOCIATED CONTENT

### Supporting Information

The Supporting Information is available free of charge on the ACS Publications website at DOI: [10.1021/acs.langmuir.9b02026](https://doi.org/10.1021/acs.langmuir.9b02026).

Intensity distribution of WPM particles at pH values 3.0 and 7.0; evolution of size of water droplets over time stabilized by curcumin or quercetin crystals and different concentrations of WPM particles; droplet size distribution and mean droplet size of water droplets stabilized by curcumin or quercetin crystals at different concentrations of WPM particles at pH 7.0; evolution of size of water droplets over time at higher water volume fractions; and interfacial shear viscosity results (PDF)

## AUTHOR INFORMATION

### Corresponding Authors

\*E-mail: [b.s.murray@leeds.ac.uk](mailto:b.s.murray@leeds.ac.uk) (B.S.M.).

\*E-mail: [A.Sarkar@leeds.ac.uk](mailto:A.Sarkar@leeds.ac.uk) (A.S.).

### ORCID

Brent S. Murray: 0000-0002-6493-1547

Anwasha Sarkar: 0000-0003-1742-2122

## Notes

The authors declare no competing financial interest.

## ACKNOWLEDGMENTS

The authors gratefully acknowledge the Engineering and Physical Sciences Research Council (EPSRC) funded Centre for Doctoral Training in Soft Matter and Functional Interfaces (SOFI), Grant ref no. EP/L015536/1, as well as Nestlé PTC Confectionery (York, U.K.) for financial support.

## REFERENCES

- (1) Dickinson, E. Food emulsions and foams: stabilization by particles. *Curr. Opin. Colloid Interface Sci.* **2010**, *15*, 40–49.
- (2) Zembyla, M.; Murray, B. S.; Sarkar, A. Water-In-Oil Pickering Emulsions Stabilized by Water-Insoluble Polyphenol Crystals. *Langmuir* **2018**, *34*, 10001–10011.
- (3) Ghosh, S.; Rousseau, D. Fat crystals and water-in-oil emulsion stability. *Curr. Opin. Colloid Interface Sci.* **2011**, *16*, 421–431.
- (4) Zembyla, M.; Murray, B. S.; Radford, S. J.; Sarkar, A. Water-in-oil Pickering emulsions stabilized by an interfacial complex of water-insoluble polyphenol crystals and protein. *J. Colloid Interface Sci.* **2019**, *548*, 88–99.
- (5) Pushpam, S. D. C.; Basavaraj, M. G.; Mani, E. Pickering emulsions stabilized by oppositely charged colloids: Stability and pattern formation. *Phys. Rev. E* **2015**, *92*, No. 052314.
- (6) Sarkar, A.; Ademuyiwa, V.; Stubbley, S.; Esa, N. H.; Goycoolea, F. M.; Qin, X.; Gonzalez, F.; Olvera, C. Pickering emulsions co-stabilized by composite protein/polysaccharide particle-particle interfaces: Impact on in vitro gastric stability. *Food Hydrocolloids* **2018**, *84*, 282–291.
- (7) Nallamilli, T.; Binks, B. P.; Mani, E.; Basavaraj, M. G. Stabilization of Pickering emulsions with oppositely charged latex particles: influence of various parameters and particle arrangement around droplets. *Langmuir* **2015**, *31*, 11200–11208.
- (8) Nallamilli, T.; Mani, E.; Basavaraj, M. G. A model for the prediction of droplet size in Pickering emulsions stabilized by oppositely charged particles. *Langmuir* **2014**, *30*, 9336–9345.
- (9) Araiza-Calahorra, A.; Sarkar, A. Pickering emulsion stabilized by protein nanogel particles for delivery of curcumin: Effects of pH and ionic strength on curcumin retention. *Food Struct.* **2019**, *21*, No. 100113.
- (10) Nicolai, T.; Britten, M.; Schmitt, C.  $\beta$ -Lactoglobulin and WPI aggregates: formation, structure and applications. *Food Hydrocolloids* **2011**, *25*, 1945–1962.
- (11) Schmitt, C.; Moitzi, C.; Bovay, C.; Rouvet, M.; Bovetto, L.; Donato, L.; Leser, M. E.; Schurtenberger, P.; Stradner, A. Internal structure and colloidal behaviour of covalent whey protein microgels obtained by heat treatment. *Soft Matter* **2010**, *6*, 4876–4884.
- (12) Dickinson, E. Biopolymer-based particles as stabilizing agents for emulsions and foams. *Food Hydrocolloids* **2017**, *68*, 219–231.
- (13) Murray, B. S.; Phisarnchananan, N. Whey protein microgel particles as stabilizers of waxy corn starch plus locust bean gum water-in-water emulsions. *Food Hydrocolloids* **2016**, *56*, 161–169.
- (14) Sarkar, A.; Kanti, F.; Gulotta, A.; Murray, B. S.; Zhang, S. Aqueous Lubrication, Structure and Rheological Properties of Whey Protein Microgel Particles. *Langmuir* **2017**, *33*, 14699–14708.
- (15) Patel, M. N.; Smith, P. G., Jr.; Kim, J.; Milner, T. E.; Johnston, K. P. Electrophoretic mobility of concentrated carbon black dispersions in a low-permittivity solvent by optical coherence tomography. *J. Colloid Interface Sci.* **2010**, *345*, 194–199.
- (16) Sahasrabudhe, S. N.; Rodriguez-Martinez, V.; O'Meara, M.; Farkas, B. E. Density, viscosity, and surface tension of five vegetable oils at elevated temperatures: Measurement and modeling. *Int. J. Food Prop.* **2017**, *20*, 1965–1981.
- (17) Murray, B. S.; Nelson, P. V. A novel Langmuir trough for equilibrium and dynamic measurements on air–water and oil–water monolayers. *Langmuir* **1996**, *12*, 5973–5976.

- (18) Murray, B. S. Equilibrium and dynamic surface pressure-area measurements on protein films at air-water and oil-water interfaces. *Colloids Surf., A* **1997**, *125*, 73–83.
- (19) Xu, R.; Dickinson, E.; Murray, B. S. Morphological changes in adsorbed protein films at the air–water interface subjected to large area variations, as observed by Brewster angle microscopy. *Langmuir* **2007**, *23*, 5005–5013.
- (20) Murray, B. S.; Cattin, B.; Schüler, E.; Sonmez, Z. O. Response of adsorbed protein films to rapid expansion. *Langmuir* **2002**, *18*, 9476–9484.
- (21) Murray, B. S. Interfacial rheology of food emulsifiers and proteins. *Curr. Opin. Colloid Interface Sci.* **2002**, *7*, 426–431.
- (22) Sarkar, A.; Zhang, S.; Murray, B.; Russell, J. A.; Boxal, S. Modulating in vitro gastric digestion of emulsions using composite whey protein-cellulose nanocrystal interfaces. *Colloids Surf., B* **2017**, *158*, 137–146.
- (23) Destribats, M.; Rouvet, M.; Gehin-Delval, C.; Schmitt, C.; Binks, B. P. Emulsions stabilised by whey protein microgel particles: towards food-grade Pickering emulsions. *Soft Matter* **2014**, *10*, 6941–6954.
- (24) Sarkar, A.; Murray, B.; Holmes, M.; Ettelaie, R.; Abdalla, A.; Yang, X. In vitro digestion of Pickering emulsions stabilized by soft whey protein microgel particles: influence of thermal treatment. *Soft Matter* **2016**, *12*, 3558–3569.
- (25) Murray, B. S. Pickering Emulsions for Food and Drinks. *Curr. Opin. Food Sci.* **2019**, *27*, 57–63.
- (26) Binks, B. P.; Horozov, T. S., *Colloidal Particles at Liquid Interfaces*; Cambridge University Press, 2006.
- (27) Schmidt, S.; Liu, T.; Rütten, S.; Phan, K.-H.; Möller, M.; Richtering, W. Influence of microgel architecture and oil polarity on stabilization of emulsions by stimuli-sensitive core–shell poly (N-isopropylacrylamide-co-methacrylic acid) microgels: Micking versus Pickering behavior? *Langmuir* **2011**, *27*, 9801–9806.
- (28) Dickinson, E. Microgels—an alternative colloidal ingredient for stabilization of food emulsions. *Trends Food Sci. Technol.* **2015**, *43*, 178–188.
- (29) Rosenholm, J. B. Evaluation of particle charging in non-aqueous suspensions. *Adv. Colloid Interface Sci.* **2018**, *259*, 21–43.
- (30) Arts, T.; Laven, J.; van Voorst Vader, F.; Kwaaitaal, T. Zeta potentials of tristearoylglycerol crystals in olive oil. *Colloids Surf., A* **1994**, *85*, 149–158.
- (31) Morrison, I. D. Electrical charges in nonaqueous media. *Colloids Surf., A* **1993**, *71*, 1–37.
- (32) Atarés, L.; Marshall, L. J.; Akhtar, M.; Murray, B. S. Structure and oxidative stability of oil in water emulsions as affected by rutin and homogenization procedure. *Food Chem.* **2012**, *134*, 1418–1424.
- (33) Picard, C.; Garrigue, P.; Tatry, M.-C.; Lapeyre, V.; Ravaine, S.; Schmitt, V.; Ravaine, V. Organization of microgels at the air–water interface under compression: Role of electrostatics and cross-linking density. *Langmuir* **2017**, *33*, 7968–7981.
- (34) Destribats, M.; Lapeyre, V.; Sellier, E.; Leal-Calderon, F.; Schmitt, V.; Ravaine, V. Water-in-oil emulsions stabilized by water-dispersible poly (N-isopropylacrylamide) microgels: Understanding anti-Finkle behavior. *Langmuir* **2011**, *27*, 14096–14107.
- (35) Destribats, M.; Wolfs, M.; Pinaud, F.; Lapeyre, V.; Sellier, E.; Schmitt, V.; Ravaine, V. Pickering emulsions stabilized by soft microgels: influence of the emulsification process on particle interfacial organization and emulsion properties. *Langmuir* **2013**, *29*, 12367–12374.
- (36) Destribats, M.; Lapeyre, V.; Sellier, E.; Leal-Calderon, F.; Ravaine, V.; Schmitt, V. Origin and control of adhesion between emulsion drops stabilized by thermally sensitive soft colloidal particles. *Langmuir* **2012**, *28*, 3744–3755.
- (37) Keal, L.; Lapeyre, V.; Ravaine, V.; Schmitt, V.; Monteux, C. Drainage dynamics of thin liquid foam films containing soft PNIPAM microgels: influence of the cross-linking density and concentration. *Soft Matter* **2017**, *13*, 170–180.
- (38) Destribats, M.; Eyharts, M.; Lapeyre, V.; Sellier, E.; Varga, I.; Ravaine, V.; Schmitt, V. Impact of pNIPAM microgel size on its ability to stabilize Pickering emulsions. *Langmuir* **2014**, *30*, 1768–1777.
- (39) Murray, B. S.; Dickinson, E. Interfacial rheology and the dynamic properties of adsorbed films of food proteins and surfactants. *Food Sci. Technol. Int.* **1996**, *2*, 131–145.
- (40) Roth, S.; Murray, B. S.; Dickinson, E. Interfacial shear rheology of aged and heat-treated  $\beta$ -lactoglobulin films: Displacement by nonionic surfactant. *J. Agric. Food Chem.* **2000**, *48*, 1491–1497.
- (41) Schmitt, V.; Ravaine, V. Surface compaction versus stretching in Pickering emulsions stabilised by microgels. *Curr. Opin. Colloid Interface Sci.* **2013**, *18*, 532–541.
- (42) Paunov, V. N.; Kralchevsky, P. A.; Denkov, N. D.; Nagayama, K. Lateral capillary forces between floating submillimeter particles. *J. Colloid & Interface Science* **1993**, *157*, 100–112.